Marine Geology 428 (2020) 106281

Contents lists available at ScienceDirect

Marine Geology

journal homepage: www.elsevier.com/locate/margo

Invited Research Article

# Sea-level fall and coastal water cooling during the Late Holocene in Southeastern Brazil based on vermetid bioconstructions

Thiago de Freitas Toniolo[a], Paulo César Fonseca Giannini[a,*], Rodolfo José Angulo[b], Maria Cristina de Souza[b], Luiz Carlos Ruiz Pessenda[c], Paula Spotorno-Oliveira[d]

[a] Instituto de Geociências, Universidade de São Paulo, Brazil
[b] Departamento de Geologia, Universidade Federal do Paraná, Brazil
[c] Centro de Energia Nuclear na Agricultura, Universidade de São Paulo, Brazil
[d] Programa de Pós-Graduação em Oceanologia, Instituto de Oceanografia, , Universidade Federal do Rio Grande, Brazil

ARTICLE INFO

*Keywords:*
Brazilian Coastal Current
La Plata Plume
Climate change
Santa Catarina coast
*Petaloconchus varians*

ABSTRACT

The relative sea-level variation curve, obtained by dating and leveling vermetid shells from northern Santa Catarina State (26.3°S), presents fall trend during all the last 4.0 cal ka BP, which matches previous results based on the same kind of indicator for the Brazilian coast between 3°S and 28°S. Chemical and isotopic analyses of 50 vermetid bioconstructions from distinct localities of south-southeastern Brazilian coast indicate possible changes in the coastal water temperature. These changes may have been caused by oscillations in the strength of Brazilian Coastal Current, which carries La Plata Plume northward, being therefore responsible for the penetration of cold and less saline water masses in the study area. This is a reasonable explanation for the scarcity of vermetid biolithites around 3.4–2.6 cal ka BP and 0.5–0 cal ka BP.

## 1. Introduction

Colonial vermetids (Mollusca, Gastropoda, Vermetidae) are largely used as paleo-sea level proxies in the Holocene (Angulo et al., 1999, 2006; Silenzi et al., 2004; Chemello and Silenzi, 2011; Spotorno-Oliveira et al., 2016). The vermetid *Petaloconchus varians* (d'Orbigny, 1839) is considered a reliable indicator of marine paleo-sea level along the Brazilian coast, due to the narrow vertical range of occurrence of its living colonies (up to 0.5 m wide in Southeast Brazil), positioned in the uppermost portion of infralittoral zone (Laborel, 1979, 1986). This characteristic associated with the aragonite composition of its shell – that allows detecting and avoiding possible contamination by secondary calcite – enable the construction of relative sea-level (RSL) curves quite accurate (Laborel, 1979, 1986; Angulo et al., 1999, 2006). Beyond that, the chemical-isotopic composition of vermetid shells, like occurs in other biogenic carbonates, may be affected by water parameters (e.g. temperature, salinity, organic nutrients), which makes their fossils potential paleoenvironmental indicators (Angulo et al., 1999; Antonioli et al., 1999; Baker et al., 2001; Silenzi et al., 2004; González-Delgado et al., 2005; Chemello and Silenzi, 2011; Jacobson et al., 2017; Shemesh et al., 2017; Areias et al., 2020).

Although Holocene *P. varians* biolithites are usually found along the Brazilian coast – from the latitude 8°S, Santo Agostinho Cape, Pernambuco State (Van-Andel & Laborel 1964) to 28°S, Santa Marta Cape, Santa Catarina State (Angulo et al., 1999) – the southernmost record of living species remains unclear (Spotorno-Oliveira et al., 2016). Present-day *P. varians* colonies are found from northeast (Ceará to Bahia states) to the southeast of Brazil (Espírito Santo to Rio de Janeiro states; Spotorno-Oliveira et al., 2012). Despite living individuals have been registered in several locations along the Rio de Janeiro State (RJ) (Spotorno-Oliveira et al., 2012), their populations disappeared or decreased on rock coasts south of Cabo Frio (RJ) in the last few decades, a fact supposedly caused by environmental factors as coastal water cooling (Laborel, 1977, 1986; Laborel and Laborel-Deguen, 1996; Breves et al., 2017). In fact, the global geographic distribution of living vermetid reefs is suggestive of sensitivity to cold waters (Safriel, 1966; Laborel, 1986; Antonioli et al., 1999; González-Delgado et al., 2005), with a minimum temperature threshold estimated to be around 14°-15 °C (Laborel, 1986, p.286; Chemello and Silenzi, 2011; Donnarumma et al., 2018). This issue enhances the interest and the significance of studying vermetids and their relation with climatic / environmental changes.

## 2. Study area and oceanographic settings

This work was carried out at São Paulo Embayment, an arc-shaped

* Corresponding author.
*E-mail address:* pcgianni@usp.br (P.C.F. Giannini).

https://doi.org/10.1016/j.margeo.2020.106281
Received 11 June 2020; Accepted 22 June 2020
Available online 25 June 2020
0025-3227/ 

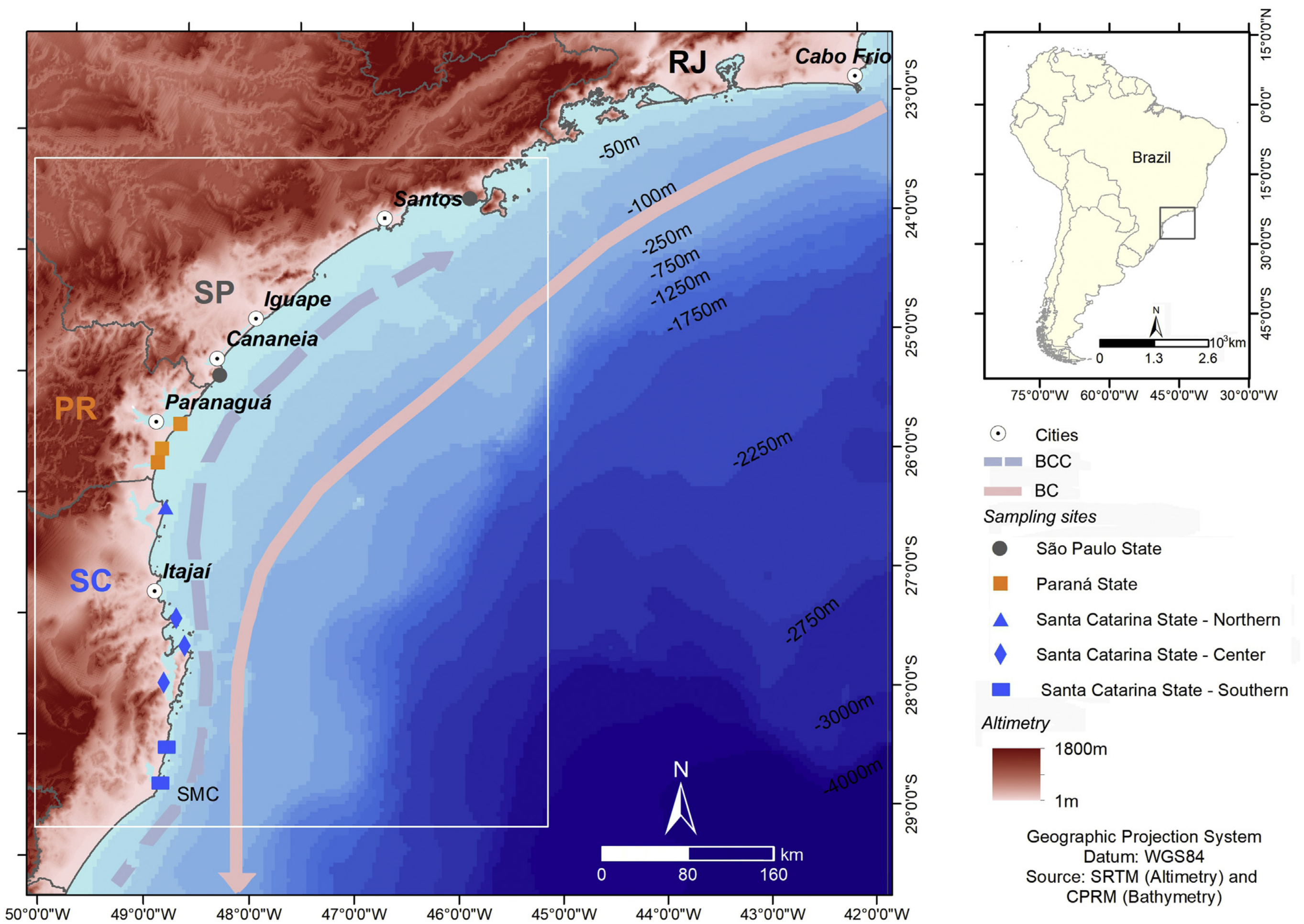


**Fig. 1.** Location of the vermetid samples analyzed (full circles, squares, triangles and diamonds) or with previous $\delta^{13}C$ data (rectangles) used here, and other places cited in this paper (circles with contour line). The study sites are comprised in the white square, along the coast of São Paulo (SP), Paraná (PR) and Santa Catarina (SC) states, the last one divided into northern, central and southern sectors. SMC: Santa Marta Cape, Laguna. BCC: Brazilian Coastal Current. BC: Brazil Current.

feature of the Brazilian coastline extending from Cabo Frio (23°S) to Santa Marta Cape (28°S) (Butler, 1970). The study sites are located in the states of São Paulo (SP; $n = 4$), Paraná (PR; $n = 14$) and Santa Catarina (SC; $n = 32$, being 23 from northern sector and nine from central sector) (Fig. 1).

The main current along the Brazilian shelf margin south of 10°S is the Brazil Current (BC) (Fig. 1), that flows southward, next to the 200 m isobath, transporting the Tropical Waters (with temperatures above 20 °C and salinity greater than 36.000), until 37°S, approximately, and with more intensity during austral summer (Silveira et al., 2000). The studied coastal area is under the influence of the Brazilian Coastal Current (BCC) (Fig. 1), which is propelled by SW winds, stronger in the winter, when it reaches up to 25°S (Souza and Robinson, 2004). Around 35°S, the La Plata River mouth takes place, and it forms a shallow and coastal body of water, called La Plata Plume (LPP), characterized by temperatures between 11 °C and 23 °C and salinity lower than 33.500 (Piola et al., 2000; Möller et al., 2008). LPP is transported to the north by BCC. The northward advance of LPP is the major responsible for continental waters influence in the study area in a regional scale (Piola et al., 2000, 2005). LPP influence is marked by a salinity and temperature transition (Emílsson, 1961) which, in summer, is located within the coast of Rio Grande do Sul (32°S), and in winter it usually reaches the mid-south coast of Santa Catarina (28°-27°S) (Piola et al., 2000, 2008; Piola and Romero, 2004; Campos et al., 2013).

La Plata River discharge, as the precipitation in southeast South America in general, is directly controlled by the intensity of the South America Monsoon System (SAMS) (Vera et al., 2006; Garreaud et al., 2009), which reached its Holocene maximum in the last 4 ka (Cruz et al., 2005; Razik et al., 2013; Bernal et al., 2016). However, freshwater supply by La Plata River discharge has a much smaller influence on the surface coastal water salinity and temperature than the seasonal variation of LPP due to BCC. In this regard, Piola et al. (2000) estimate that the effect of the La Plata River flow increase recorded during the anomalous rainfall of the 1983 El Niño year was about five times lesser than the average effect of LPP seasonal variation.

The influence of run-off by other rivers, beyond La Plata River, is hindered in the study area, at the regional scale, due to its geomorphological configuration: the main drainages in this portion of south / southeast Brazil are comprised in the Paraná River Basin, which ultimately flows to west into the La Plata River (Emílsson, 1956, 1961; Almeida, 1964; Almeida and Carneiro, 1998; Villwock et al., 2005; Dominguez, 2009). The majority of rivers that flow towards the sea on the studied stretch of coast have small drainage areas (less than 1000 km$^2$), and most of the few larger rivers (eg. Ribeira de Iguape River, Tubarão River) flow into semi-enclosed lagoon-estuarine systems (Santos, Cananeia-Iguape, Paranaguá and Laguna: Fukumoto et al., 2004, Giannini et al., 2009, Angulo et al., 2009 and Hesp et al., 2009, respectively), where the freshwater supply to the sea in constrained by waves and flood tide currents acting at the inlets. Despite this, the register of lower values of salinity in shallow inner shelf waters around Santos estuary and Paranaguá and Cananeia-Iguape (Ribeira de Iguape River mouth region) lagoonal-estuarine complexes (Freitas and

Muelbert, 2004; Piola et al., 2000; Piola and Romero, 2004) allows to suspect the influence of local freshwater on the coastal waters of these regions. South of the Ribeira do Iguape River mouth (Iguape; Fig. 1), the largest river in the study area is the Itajaí-Açu, located in the north of Santa Catarina (Itajaí; Fig. 1), whose plume has an average range of less than 10 km, without directly affecting the waters closest to the coastline (Schettini, 2002).

The outflow of local fresh water into the sea is larger during the spring-summer, when the precipitation is higher (Cruz et al., 2005; Vera et al., 2006) and swell waves from NE and E are prevalent, than during the fall-winter, when, inversely, the fluvial supply diminishes and long period waves from S and SE becomes dominant (Pianca et al., 2010; Colonese et al., 2017).

Both the northernmost and the southernmost limit of the São Paulo Embayment (Fig. 1) are localities subjected to coastal upwelling, related to abrupt changes in the coastline direction and the action of winds from NE during summer (Campos et al., 2013; Mazzini and Barth, 2013). The upwelling in Cabo Frio is the strongest of Brazil, influencing coastal waters along more than a hundred kilometers (Castelão and Barth, 2006), but without affecting the vermetid sampling points of this study, shown in Fig. 1 (Franchito et al., 2008; Palma and Matano, 2009). The influence of Santa Marta Cape upwelling, in counterpart, is restricted to the vicinities of Laguna, in a radius of a few tens of kilometers (Möller et al., 2008; Campos et al., 2013).

Although the lack of systematic isotopic analyses of water masses in the study area, it is presumed, that, in a regional scale, by analogy with other similar contexts (Mook and Tan, 1991; Chanton and Lewis, 1999; Venancio et al., 2014; Benetti et al., 2017), the continental waters of LPP are depleted in $\delta^{18}O$ and $\delta^{13}C$ (in the dissolved inorganic carbon) with respect to the evaporative and nutrient-poor surrounding Tropical Waters. At Santa Marta Cape (28°S), it is also possible that the nutrient-rich upwelling waters, being originated from less evaporative deep waters, have lower $\delta^{18}O$ and $\delta^{13}C$ (Pierre et al. 1991, Venancio et al., 2014, Benetti et al., 2017) in comparison to the Tropical Waters.

## 3. Materials and methods

35 samples of vermetid colonies collected along the coast of São Paulo, Paraná, and Santa Catarina States were analyzed in this work as for geochronology ($^{14}C$ ages) and chemical-isotopic composition ($\delta^{18}O$, $\delta^{13}C$ and Sr/Ca). From these 35 samples, 18 were found in situ in São Francisco do Sul (northern Santa Catarina State), so they also were leveled during field trip using topographic equipment in order to determine the paleo-sea level (this method is fully explained in the section 3.2).

Besides these 35 samples, this work also performed isotopic and Sr/Ca analyzes in 11 samples from São Paulo, Paraná and Santa Catarina states, collected and dated by Angulo et al. (2006) and four samples from Palhoça (central region of Santa Catarina State), collected and dated by Angulo et al. (2020).

### 3.1. Paleo-sea level determination

According to Laborel (1986) to determine the paleo-sea level, the altimetry difference between the top of the in situ fossil vermetid and the top of the living vermetids must be measured, using topographic equipment, in the same cross section of the littoral (which ensures that surf conditions are nearly the same in both fossil and living vermetids). This method has been largely used to obtain very reliable and consistent paleo-sea level curves for the last six thousand years in the Brazilian coast (Angulo et al., 1999, 2006, 2015).

Because no living vermetids were found in the study area, the estimating of RSL from the fossil samples in this work required the use of another living organism, able to indicate the level that vermetids would occupy today. The species we used as reference was *Phragmatopoma caudata* Krøyer in Mörch, 1863, a polychaeta that builds its colonies by agglutination of sand and granules (Angulo et al., 1999). Using this reference, height measurements of the 18 vermetid colonies found in São Francisco do Sul (SC) were made and then collected samples from each one.

According to Laborel (1979, 1986) vermetid bioconstructions can provide paleo-sea level reconstructions with precision ranging between ± 0.1 to ± 1.0 m depending on tidal range, wave exposition and bedrock morphology. Precision of ± 0.5 m was adopted here considering that: (a) São Francisco do Sul is under micro-tidal regime, that diminish the width of vermetid constructions (Laborel, 1986); (b) the reconstructions were performed using the main top-level of living *P. caudata* (used as vermetid homologous) avoiding over elevated constructions by the wave run-up; (c) the present wave exposition of living bioconstructions is similar to the one inferred for the fossil colonies; and (d) the vermetid colonies were differentiate according bedrock morphology. At tidal ponds and narrow vertical cavities, the vermetid bioconstructions can be over elevated by the effect of wave run-up (Delibrias and Laborel, 1969). To verify this effect at São Francisco do Sul, five vermetid colonies (F6.1 to F6.5) found in a vertical narrow cavity and spreading across 1.89 m were collected, within the total of 18 samples at this place.

### 3.2. Preparation and analysis of vermetid samples

All samples (50 in total) were subjected to surface cleaning with a brush under flowing water and then immersed in $H_2O_2$ 30 vol for at least 48 h to remove all organic matter that could generate contamination and thus affect the chemical / isotopic and dating results. After that, colonies were mechanically disaggregated, and fragments of vermetid shells were selected under stereoscopic microscope. This turned out to be the most efficient method to avoid contamination by cements (mainly calcite and clay minerals) in the subsequent analysis.

Each sample was then dried, powdered and homogenized in an agate mortar. An aliquot from each one was pulled out for X-ray Diffraction (XRD) in order to verify if in any sample there would be significant amounts ($>$ 5%) of calcite and clay minerals that could alter the results of dating or chemical / isotopic composition. 13 of the samples were submitted to petrographic analysis, and among these, two samples were examined by SEM/EDS analysis to verify that the percentages of other types of carbonate (not the vermetid shell) and clay minerals were really low.

From each powdered sample, three aliquots were withdrawn for: **1.** AMS $^{14}C$ dating in the Poznan Radiocarbon Laboratory, Adam Mickiewicz University, Poland. **2.** $\delta^{13}C$ and $\delta^{18}O$ quantification by isotope-ratio mass spectrometry in the Stable Isotope Laboratory (LIE) at the Instituto de Geociências of Universidade de São Paulo (USP), Brazil. For each measurement, ~200 μg of powder was drilled from the sample and analyzed with an online, automated, Gas Bench system linked to a Finnigan Delta Plus Advantage mass spectrometer. Ratios were determined on evolved $CO_2$ gas released from carbonate minerals by reaction with orthophosphoric acid at 72 °C. Accuracy of the analysis was ± 0.02‰ for $\delta^{18}O$ and ± 0.03‰ for $\delta^{13}C$. **3.** Sr/Ca obtainment by inductively coupled plasma optical emission spectrometry (ICP-OES) with the standard solution 111,355 - ICP Certipur® 1000 mg/l, performed in a Spectro Arcos® equipment at the Central Analítica of Instituto de Química of USP, Brazil. Samples were dissolved with concentrated HCl and 100 °C heating. Analyses were taken after dilution in 50 ml of distillated water, with applied power of 1400 W.

The AMS $^{14}C$ dating results were converted into calibrated years before present (cal a BP), with error of two standard deviations (2σ), using in the CALIB REV7.0.1 program the calibration curve Marine 13 (available in http://radiocarbon.pa.qub.ac.uk/calib). The Sr/Ca ratios are expressed in $10^{-3}$ mol/mol (mmol/mol) and the $\delta^{13}C$ and $\delta^{18}O$ values are referred to Vienna Pee Dee Belemnite standard value (V-PDB) and expressed in parts per mille (‰). For the linear trends, the correlation coefficient (r) and the significance level (*p*-value) calculated

**Table 1**
Location, radiocarbon ages, paleo-sea levels and geochemical data of *P. varians* samples studied in this paper.

| Sample code | Location | Latitude (UTM) | Laboratory reference | $^{14}C$ age (a BP) | $^{14}C$ age (cal a BP) (2σ) | Paleo-sea level (m) | $\delta^{18}O$ (V-PDB) ‰ | $\delta^{13}C$ (V-PDB) ‰ | Sr/Ca (mmol/mol) |
|---|---|---|---|---|---|---|---|---|---|
| CENA-135 | Morro da Tapera, Ilha do Cardoso (SP) | 7,214,476 | CENA-135 | 1890 ± 60* | 1549–1294* | – | −0.54 | 2.14 | 2.46 |
| CENA-136 | Morro da Tapera, Ilha do Cardoso (SP) | 7,214,476 | CENA-136 | 500 ± 60* | 244–0* | – | −0.36 | 0.81 | 2.13 |
| SB-01 | São Sebastião (SP) | 7,367,305 | Poz-75,757 | 920 ± 30 | 601–478 | – | −0.21 | 1.28 | 2.36 |
| SP-02 | Morro da Tapera, Ilha do Cardoso (SP) | 7,214,476 | Poz-75,665 | 1655 ± 30 | 1283–1152 | – | 0.17 | 0.96 | 2.43 |
| CENA-137 | Ilha dos Currais (PR) | 7,150,806 | CENA-137 | 490 ± 60* | 240–0* | – | −0.60 | 1.54 | 2.22 |
| CENA-138 | Ilha dos Currais (PR) | 7,150,806 | CENA-138 | 1280 ± 60* | 925–687* | – | −0.57 | 1.17 | 2.20 |
| CENA-140 | Morro do Farol, Caiobá (PR) | 7,139,039 | CENA-140 | 4750 ± 70* | 5222–4826* | – | −0.61 | 0.47 | 2.25 |
| CENA-141 | Morro do Farol, Caiobá (PR) | 7,139,039 | CENA-141 | 5300 ± 70* | 5845–5513* | – | −0.86 | 0.70 | 2.13 |
| CENA-142 | Morro do Farol, Caiobá (PR) | 7,139,039 | CENA-142 | 2470 ± 70* | 2295–1939* | – | −0.65 | 1.17 | 2.85 |
| GSC-5251 | Ponta das Conchas, Ilha do Mel (PR) | 7,172,341 | GSC-5251 | 790 ± 80* | 528–276* | – | −0.54 | 0.61 | 2.15 |
| GSC-5255 | Ponta das Conchas, Ilha do Mel (PR) | 7,172,341 | GSC-5255 | 3500 ± 60* | 3520–3223* | – | −1.46 | 0.59 | 2.24 |
| PR-01 | Morro das Encantadas, Ilha do Mel (PR) | 7,169,847 | Poz-75,650 | 1945 ± 30 | 1582–1397 | – | 0.21 | 2.42 | 2.44 |
| PR-02 | Praia de Fora, Ilha do Mel (PR) | 7,172,484 | Poz-75,653 | 2945 ± 35 | 2808–2660 | – | −0.54 | 0.65 | 3.03 |
| PR-03 | Ilha do Mel (PR) | 7,171,649 | Poz-75,654 | 1990 ± 30 | 1665–1460 | – | −1.00 | 0.88 | 2.05 |
| PR-04 | Morro das Encantadas, Ilha do Mel (PR) | 7,169,847 | Poz-75,655 | 1460 ± 30 | 1092–922 | – | −0.67 | 1.12 | 2.18 |
| PR-05 | Ponta das Conchas, Ilha do Mel (PR) | 7,172,341 | Poz-75,990 | 325 ± 30 | 0–0 | – | −1.02 | 0.70 | 2.58 |
| PR-08 | Morro das Encantadas, Ilha do Mel (PR) | 7,169,847 | Poz-75,657 | 3975 ± 35 | 4084–3856 | – | −0.33 | 2.07 | 2.74 |
| PR-09 | Morro das Encantadas, Ilha do Mel (PR) | 7,169,847 | Poz-75,659 | 600 ± 30 | 300–137 | – | −0.85 | 0.16 | 2.48 |
| F6.1(2.5) | Morro do Forte–Itaguaçu, SFS (SC-N) | 7,096,080 | Poz-62,473 | 3575 ± 30 | 3554–3378 | 2.45 | 0.01 | 0.83 | 2.17 |
| F6.2(2.0) | Morro do Forte–Itaguaçu, SFS (SC-N) | 7,096,080 | Poz-62,659 | 1855 ± 30 | 1498–1315 | 2.05 | −0.18 | 1.42 | 3.06 |
| F6.3(0.9) | Morro do Forte–Itaguaçu, SFS (SC-N) | 7,096,080 | Poz-62,474 | 2080 ± 30 | 1752–1553 | 0.94 | −0.25 | 0.48 | 2.48 |
| F6.4(0.7) | Morro do Forte–Itaguaçu, SFS (SC-N) | 7,096,080 | Poz-62,475 | 1845 ± 30 | 1485–1303 | 0.71 | −0.12 | 0.39 | 2.52 |
| F6.5(0.6) | Morro do Forte–Itaguaçu, SFS (SC-N) | 7,096,511 | Poz-62,476 | 1450 ± 30 | 1075–917 | 0.56 | 0.07 | 0.76 | 2.26 |
| F6.6(0.7) | Morro do Forte–Itaguaçu, SFS (SC-N) | 7,102,413 | Poz-62,660 | 1470 ± 30 | 1109–930 | 0.71 | −0.30 | 1.11 | 2.10 |
| GX-14060 | Ponta da Enseada, SFS (SC-N) | 7,097,382 | GX-14060 | 4015 ± 90* | 4276–3761* | – | −0.57 | 0.87 | 3.13 |
| P5(0.5) | Prainha (north), SFS (SC-N) | 7,096,080 | Poz-62,472 | 1315 ± 40 | 943–756 | 0.46 | −0.03 | 1.39 | 2.40 |
| S1(0.6) | Praia da Saudade, SFS (SC-N) | 7,096,080 | Poz-62,459 | 2005 ± 35 | 1683–1478 | 0.59 | 0.24 | 1.19 | 2.08 |
| S2.1(2.6) | Praia da Saudade, SFS (SC-N) | 7,096,080 | Poz-62,460 | 3970 ± 30 | 4074–3863 | 2.64 | 0.11 | 1.22 | 2.27 |
| S2.2(2.4) | Praia da Saudade, SFS (SC-N) | 7,096,080 | Poz-62,461 | 3880 ± 30 | 3954–3734 | 2.37 | 0.13 | 1.13 | 2.16 |
| S2.3(1.5) | Praia da Saudade, SFS (SC-N) | 7,096,080 | Poz-62,462 | 2675 ± 30 | 2463–2297 | 1.47 | 0.07 | 0.90 | 3.52 |
| S2.4(1.4) | Praia da Saudade, SFS (SC-N) | 7,096,080 | Poz-62,464 | 2730 ± 30 | 2592–2331 | 1.37 | 0.02 | 0.69 | 3.26 |
| S2.5(1.1) | Praia da Saudade, SFS (SC-N) | 7,102,413 | Poz-62,465 | 2625 ± 30 | 2397–2189 | 1.13 | 0.04 | 0.84 | 2.78 |
| S2.6(0.9) | Praia da Saudade, SFS (SC-N) | 7,102,413 | Poz-62,466 | 2320 ± 40 | 2051–1825 | 0.94 | 0.20 | 1.10 | 3.08 |
| S2.7(0.8) | Praia da Saudade, SFS (SC-N) | 7,102,413 | Poz-62,468 | 2150 ± 30 | 1833–1634 | 0.81 | 0.31 | 1.02 | 2.73 |
| S2.8(0.6) | Praia da Saudade, SFS (SC-N) | 7,100,369 | Poz-62,469 | 1775 ± 30 | 1385–1262 | 0.62 | −0.14 | 0.60 | 2.30 |
| S3(2.3) | Praia da Saudade, SFS (SC-N) | 7,100,369 | Poz-62,470 | 3680 ± 30 | 3685–3490 | 2.32 | −0.02 | 1.98 | 3.55 |
| S4(0.6) | Praia da Saudade, SFS (SC-N) | 7,096,080 | Poz-62,471 | 2080 ± 30 | 1752–1553 | 0.63 | −0.17 | 1.01 | 2.06 |
| SC-02 | Ponta da Enseada, SFS (SC-N) | 7,097,382 | Poz-75,660 | 1410 ± 30 | 1040–896 | – | −0.88 | 1.71 | 2.04 |
| SC-03 | Ponta da Enseada, SFS (SC-N) | 7,097,382 | Poz-75,661 | 1295 ± 30 | 915–758 | – | −0.67 | 1.18 | 2.11 |
| U7.1 | Ubatuba–Itaguaçu, SFS (SC-N) | 7,102,413 | Poz-62,661 | 2750 ± 30 | 2612–2342 | – | −0.01 | 0.60 | 2.79 |
| U7.3 | Ubatuba–Itaguaçu, SFS (SC-N) | 7,102,413 | Poz-62,479 | 2265 ± 30 | 1966–1789 | – | −0.17 | 1.83 | 4.95 |
| Pnh2 | Praia de Pinheira, Palhoça (SC-C) | 6,913,254 | CENA-1005 | 2310 ± 70** | 2112–1753** | – | 0.40 | 1.60 | 2.26 |
| Pnh3 | Praia de Pinheira, Palhoça (SC-C) | 6,913,254 | CENA-1006 | 1500 ± 70** | 1216–914** | – | 0.36 | 1.67 | 1.90 |
| Pnh4 | Praia de Pinheira, Palhoça (SC-C) | 6,913,254 | CENA-1007 | 1200 ± 70** | 898–640** | – | 0.33 | 2.05 | 2.37 |
| Pnh5 | Praia de Pinheira, Palhoça (SC-C) | 6,913,254 | CENA-1008 | 3860 ± 80** | 4054–3611** | – | 0.44 | 2.20 | 2.92 |
| GX-14061 | Praia de Armação, Florianópolis (SC-C) | 6,928,177 | GX-14061 | 1045 ± 75* | 723–501* | – | −1.00 | 1.52 | 2.07 |
| PI-01 | Praia de Pinheira, Palhoça (SC-C) | 6,913,254 | Poz-75,649 | 1650 ± 30 | 1281–1145 | – | −0.56 | 1.92 | 2.32 |
| SC-01 | Bombinhas headland (SC-C) | 6,994,883 | Poz-75,758 | 2725 ± 30 | 2570–2326 | – | −0.65 | 1.73 | 2.53 |
| SCP-01 | Praia de Pinheira, Palhoça (SC-C) | 6,913,254 | Poz-75,663 | 2670 ± 30 | 2459–2294 | – | 0.40 | 1.97 | 2.20 |
| SCP-03 | Praia de Pinheira, Palhoça (SC-C) | 6,913,254 | Poz-75,664 | 1230 ± 30 | 870–690 | – | 0.18 | 1.92 | 2.21 |

Notes: all data from the present study, except those marked with * (Angulo et al., 2006) and ** (Angulo et al., 2020); (Poz) Poznań Radiocarbon Laboratory; (CENA) Laboratório de $^{14}C$ do Centro de Energia Nuclear na Agricultura, Campus de Piracicaba, Universidade de São Paulo; (GSC) Radiocarbon Dating Laboratory, Geological Survey of Canada; (GX) Krueger Enterprises Inc. Geochron Laboratories Division; (SP) São Paulo State; (PR) Paraná State; (SFC) São Francisco do Sul; (SC-N) northern Santa Catarina State; (SC-C) central Santa Catarina State.

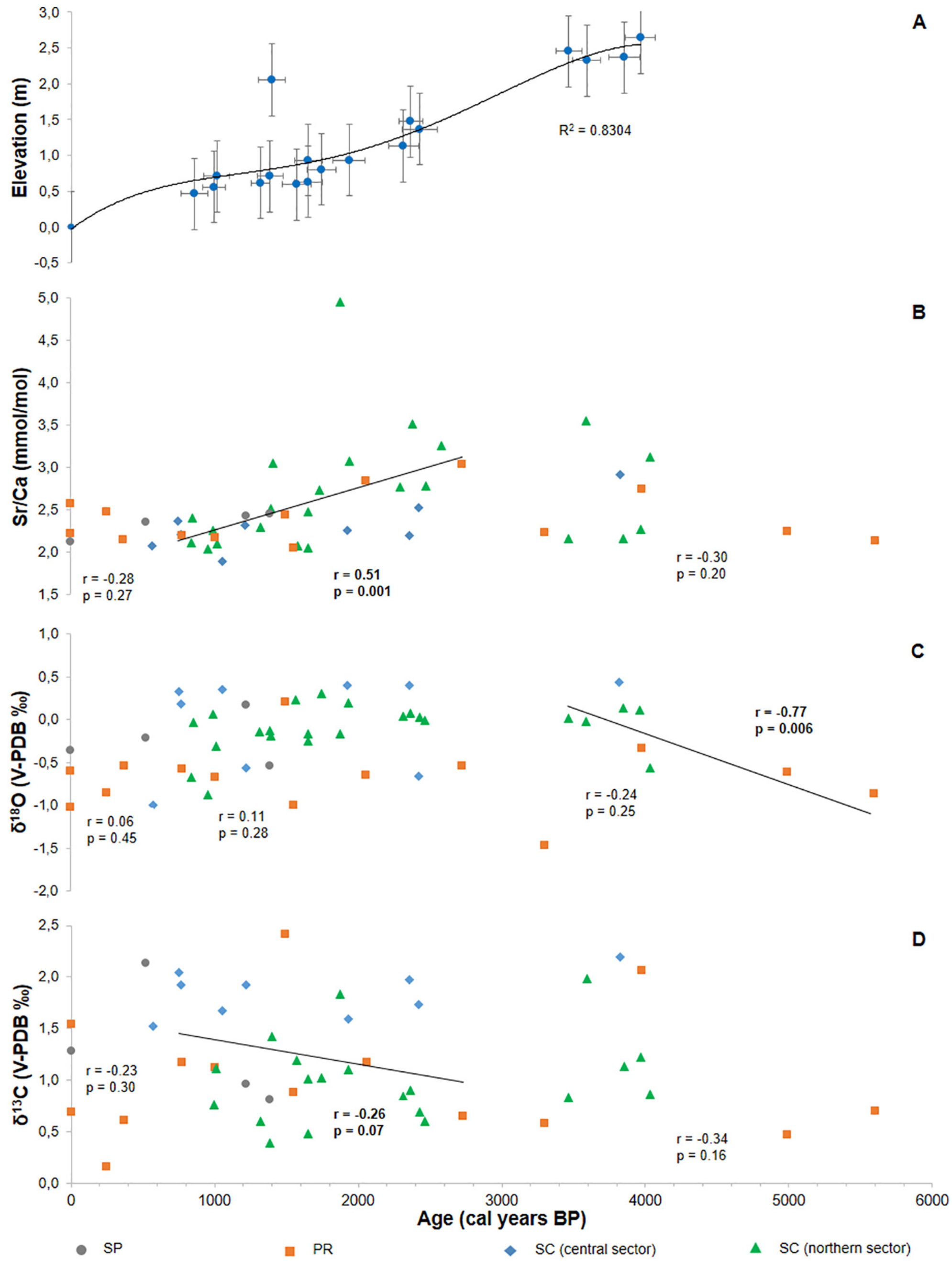


**Fig. 2.** Scatterplots of all the paleo-sea level, $\delta^{18}O$, $\delta^{13}C$ and Sr/Ca data of the vermetid samples analyzed in this work. A: RSL variation (forth degree polynomial) curve from São Francisco do Sul (SC) based on 18 vermetids data (vertical error of ± 0.5 m); B: Sr/Ca values with linear trends, correlation coeficient (r) and the significance level (p); C: $\delta^{18}O$ values; D: $\delta^{13}C$ values. B, C and D are based on the 50 vermetid samples from the São Paulo (SP), Paraná (PR) and Santa Catarina (SC) states listed in Table 1.

by the one-tailed Student's T score are presented in the graphs. Following Dahiru (2008), the borderline p-value of 0.1 was adopted as a criterion for representing or not the regression lines in these graphs.

## 4. Results

The 18 paleo-sea level data from the samples found in situ in São Francisco do Sul, the geochronological and chemical-isotopic data from the 35 samples collected in this study (including the São Francisco do Sul ones) and the chemical-isotopic data from the 11 samples collected by Angulo et al. (2006) and the four samples collected by Angulo et al. (2020)) are summarized in Table 1 and Fig. 2.

The fossil bioconstructions found in situ on rocky shores of São Francisco do Sul (Fig. 3A), when analyzed in thin sections under the petrographic microscope, consist mainly of vermetid shells, primary porosity and siliciclastic grains in similar amounts (Fig. 3B). The vermetid shells present the diagnostic features of *P. varians* (Keen, 1961; Laborel, 1986) like reticulated external ornamentation and internal columellar lamellae (Fig. 4A-C). In section the shells have about 1.2 mm of internal diameter and the wall is about 0.2 mm thick and composed by several layers of radially arranged aragonite crystals (Fig. 4D). The paleo-sea level obtained in fieldwork, as well as the chemical and isotopic data of vermetid shells (Table 1) are detailed next.

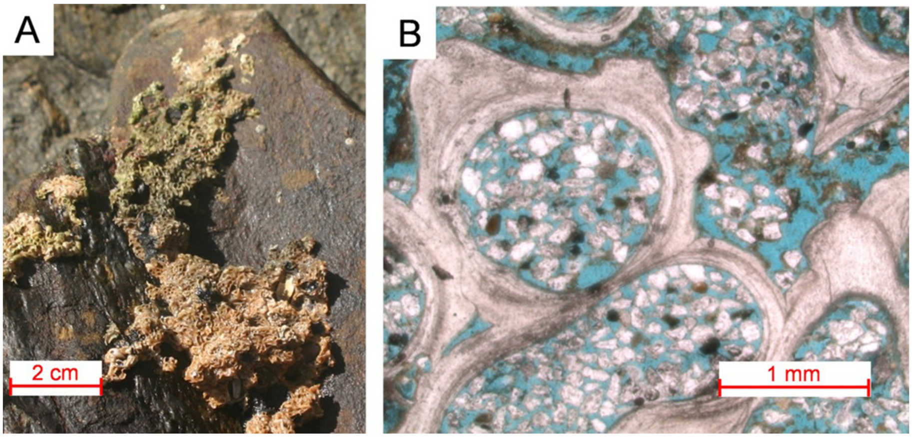


**Fig. 3.** *Petaloconchus varians* from São Francisco do Sul (Santa Catarina State). A: fossil colony inlaying granitoid rock at Morro do Forte – Itaguaçu; B: thin section of a sample (F6.1(2.5)) containing large amounts of siliciclastic grains (~25% in area) and primary porosity (~30% in area); photomicrography under petrographic microscope with uncrossed polarizers.

### 4.1. Sea-level variation curve

The vermetid *P. varians* leveling and dating data from São Francisco do Sul allowed the construction of a forth degree polynomial curve (intercepted in (0,0)) which reveals smooth decreasing trend (Fig. 2A) along the last 4.0 cal ka BP, with maximum elevation of +2.9 m around 4.0 cal ka BP (oldest sample), minimum of +0.5 m at 0.9 cal ka BP (youngest sample) and average sea level falling velocity of 6.6 cm per century. In this data set it is also possible to notice two time ranges without samples: between 0.9 and 0 cal ka BP and from 3.5 to 2.4 cal ka BP, approximately (Fig. 2A).

The paleo-sea level of the vermetid colonies collected at a vertical narrow cavity in São Francisco do Sul (samples F6.1 to F6.5) ranges from +2.45 to +0.56 m (Fig. 5) and the dated samples give ages from 3378 to 3554 to 917–1075 cal a BP. The age deceased with altitude, except for the sample at +2.05 m (F6.2), which presents similar age of the sample at +0.71 m (F6.4).

### 4.2. Geochemical analysis

The scatterplots of all the geochemical and $^{14}C$ data set of vermetids from Santa Catarina to São Paulo (Fig. 2B, C and D) reveals a period of samples absence between approximately 3.3 and 2.7 cal ka BP. This period is longer (3.4 to 2.6 cal ka BP) when considering only the southernmost (Santa Catarina) samples. In this same region, there is also a period of shortage of vermetid samples after 0.5 cal ka BP. Linear trends were calculated to three time intervals (Fig. 2B, C and D): before the beginning of vermetid absence period; between the end of absence period and the beginning of period of shortage in Santa Catarina; and during the period of shortage.

The scatterplots of all $\delta^{18}O$ and $\delta^{13}C$ (Fig. 2C and D) values as function of age show large data dispersion. In the time interval with the highest concentration of data (33 from the total of 50), between 2.7 and 0.7 ka BP, linear variation trends have low r and confidence level ($r = 0.11$ and $p = .28$ for $\delta^{18}O$) or high confidence level but not so much high r ($r = 0.26$ and $p = .07$ for $\delta^{13}C$). In the time range older than 3.3 ka BP, with lower number of samples (ten), the linear trends have $p$-value $> .1$ ($r = 0.34$ and $p = .16$, for $\delta^{13}C$; $r = 0.24$ and $p = .25$

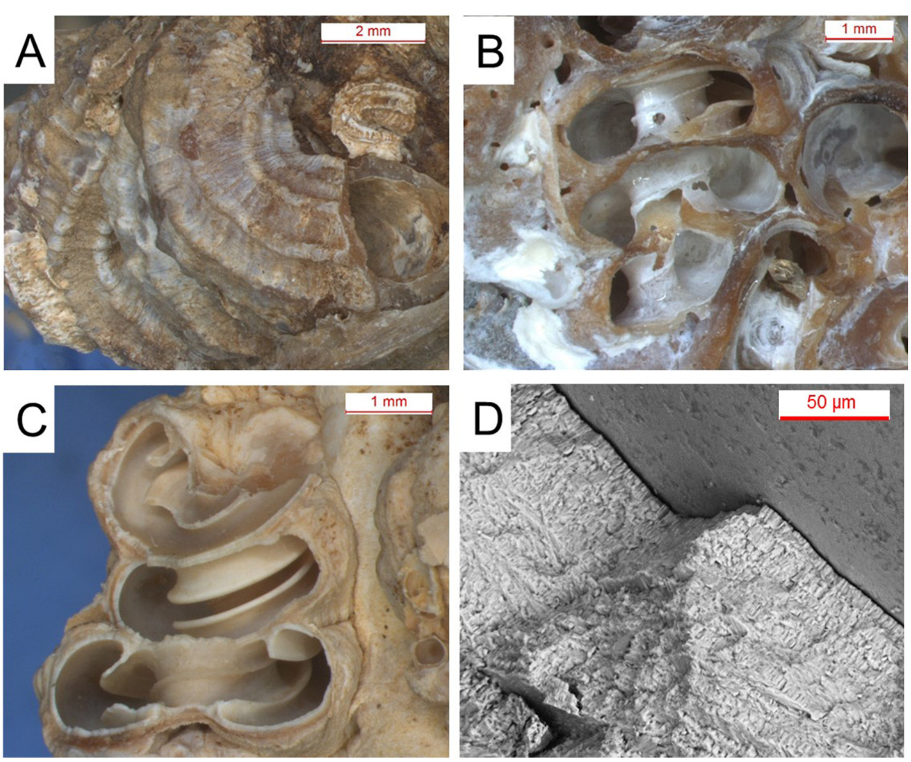


**Fig. 4.** *Petaloconchus varians* shells in detail. A: reticulated external ornamentation (sample SB-01, São Sebastião, São Paulo State); B: regularly coiled specimen showing columella (sample F6.6(0.7), São Francisco do Sul, Santa Catarina State); C: internal columellar lamellae projecting from the columellar wall of the tube (sample GX-16061, Florianópolis, Santa Catarina State); D: vermetid shell wall revealing structure of concentric layers of radially disposed aragonite crystals (sample CENA 141, Caiobá, Paraná State); on the upper right, micrite calcite fills the tube. A and B: photomicrographs under stereoscopic magnifying glass; C: photomicrographs under the petrographic microscope with uncrossed polarizers; D: SEM image, using backscattered electrons detector.

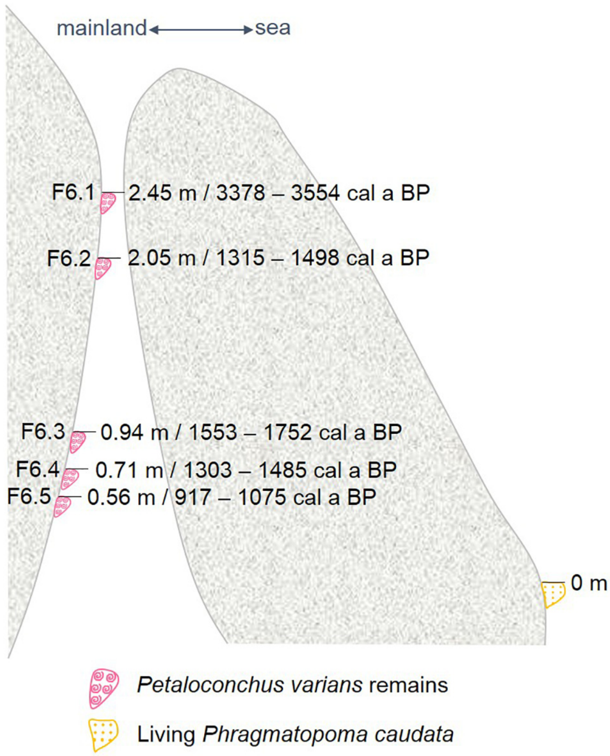


**Fig. 5.** Schematic section representing the space-time distribution of five vermetid colonies found on a same vertical narrow cavity at São Francisco do Sul.

for $\delta^{18}O$), but clearly there is an outlier in $\delta^{18}O$ data. Eliminated this outlier, ie, considered only the nine oldest samples, the linear trend to elevation over time of $\delta^{18}O$ becomes statistically more significant ($r$ = 0.77 and $p$ = .006). The most significant linear trend found over time ($r$ = 0.51 and $p$ = .001) is the decreasing Sr/Ca from 2.7 to 0.7 cal ka AP (Fig. 2B). Before and after this time interval, Sr/Ca values show linear trends to increase over time, with lower significance levels due to the reduced number of samples (Fig. 2B).

## 5. Discussion

### 5.1. Sea-level variation

The RSL variation curve of São Francisco do Sul (SC) shows smooth fall trend from 2.9 ± 0.5 m at 4.0 cal ka BP until the modern sea level (zero), which is in accordance with the paleo-sea level data obtained from vermetids and compiled by Angulo et al. (2006) for the Brazilian coastal region between 3°S and 28°S (Fig. 6). However, in a more detailed approach, it is noticeable that in the last 2.5 ka BP the RSL variation curve of São Francisco do Sul (26.3°S) is about 0.5 and 0.8 m below that from Pernambuco (3°S) to Paraná (25.5°S) states, and is very similar to the curve from southern Santa Catarina state (28°S). In fact, Angulo et al. (2006) already noticed the difference among RSL variation curves from 28°S and the further northern locations.

The distribution of the vermetid colonies (samples F6.1 – F6.5) and bedrock morphology of the narrow cavity where they were found in (Fig. 5) suggest that around 3378–3554 cal a BP paleo-sea level was +2.45 m and the cavity was submerged. From 1553 to 1752 to 917–1075 cal a BP when paleo-sea level declined from 0.94 m to 0.56 m the cavity remains above sea-level under the effect of wave run-up, which allowed vermetid (sample F6.2) to live 1.34 m over his regular living zone (F6.4). Considering the sea-level curve obtained at São Francisco do Sul (Fig. 2) is clear that sample F6.2 is over elevated, which confirms the effect of wave run-up on narrow cavities as postulated by Laborel (1979, 1986).

Description of bedrock morphology and hydrodynamic conditions, therefore, are significant to estimate the precision of paleo-sea level reconstructions. This approach may also be applied for other species used as paleo-sea level indicators as *Tetraclita stalactifera* or *Tesseropora atlantica* (Angulo and Souza, 2014) or for *P. caudata*, used as homologous of vermetids where they are missing at present days (Angulo et al., 1999 and this paper).

### 5.2. Palaeoceanographic conditions

The variation ranges of $\delta^{13}C$ and $\delta^{13}O$ in the studied samples (2.4 and 2.0‰, respectively) is larger than those found by González-Delgado et al. (2005) in recent vermetid samples of a same locus and age (0.6‰ to both $\delta^{13}C$ and $\delta^{13}O$), what means that part of them can result from environmental changes.

#### 5.2.1. Spatial variation

The boxplot and dotplot graphs of $\delta^{13}C$ values at each locality (Fig. 7) show that the interquartile range and/or the median value increase from Paraná State to north (São Paulo State) as well to south (southern sector of Santa Catarina State). The highest $\delta^{13}C$ values are found in the southern Santa Catarina whose interquartile range is the only one that does not overlap with any other.

Since continental waters present more depleted $\delta^{13}C$ values than marine waters (Newton and Bottrell, 2007) and LPP is the most important source of continental waters in the study area in a regional scale (Piola et al., 2000, 2005), the decreasing influence from south to north of LPP (Piola et al., 2000, 2005) would imply an enrichment trend of

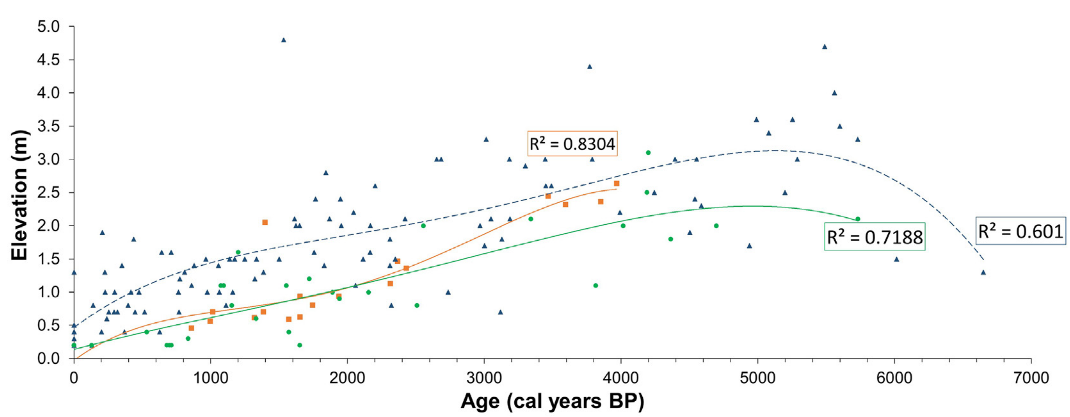


**Fig. 6.** RSL variation curve from Brazilian coast based on 158 vermetid samples. Triangles and dashed line: data from the Brazilian coast between Pernambuco (3°S) and Paraná (25.5°S) (Angulo et al., 2006). Circles and green line: data from southern Santa Catarina State (28°S) (Angulo et al., 2006). Squares and orange line: São Francisco do Sul (26.3°S) (this work). (For interpretation of the references to colour in this figure legend, the reader is referred to the web version of this article.)

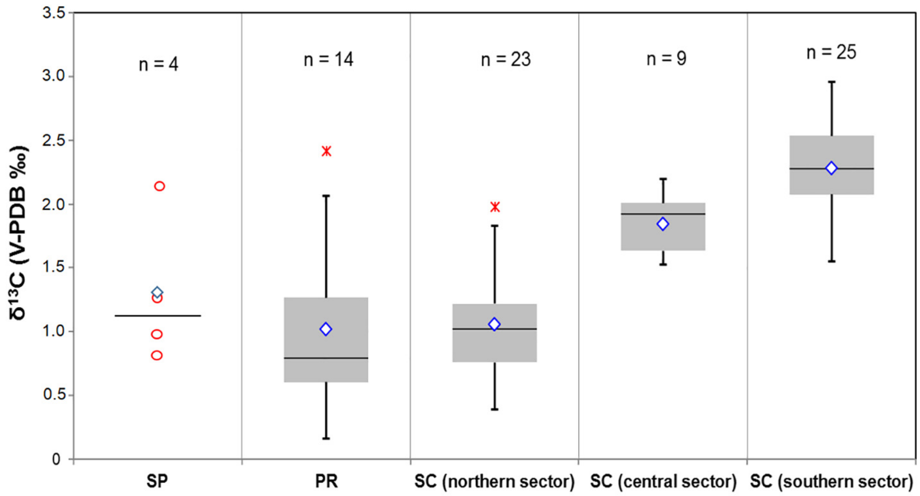


**Fig. 7.** Dotplot and boxplots of $\delta^{13}C$ values for vermetid samples from the South / Southeast Brazilian coast. Values from the southern sector of Santa Catarina State according to Angulo et al. (1999). Red circle represents individual value, gray box, the interquartile range, horizontal trace, the median, diamond represents the mean and asterisk, outlier. SP: São Paulo State, PR: Paraná State, SC: Santa Catarina State. (For interpretation of the references to colour in this figure legend, the reader is referred to the web version of this article.)

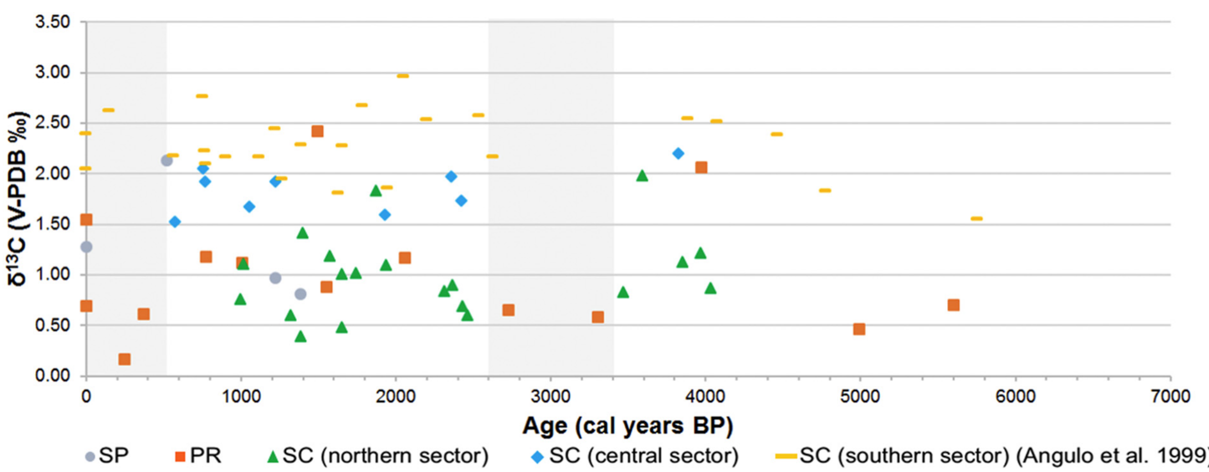


**Fig. 8.** Scatterplot between $\delta^{13}C$ values and median calibrated age for 75 vermetid samples from the South / Southeast Brazilian coast (50 data from this work and the 25 data from the southern section of Santa Catarina State from Angulo et al., 1999). Shaded areas delimit periods of scarcity of samples in the entire coast of Santa Catarina State. SP: São Paulo State, PR: Paraná State, SC: Santa Catarina State.

$\delta^{13}C$ from Santa Catarina to São Paulo. However, when comparing $\delta^{13}C$ data obtained in this work with the data presented by Angulo et al. (1999) in Laguna-Imbituba region (southern Santa Catarina) (Fig. 8), we can notice that these authors found higher mean values than those obtained in this study, which is also evident in the boxplot-dotplot graph of the $\delta^{13}C$ values at each region of the São Paulo Embayment (Fig. 7). This graph shows an inversion trend, in relation to that predicted with basis only on the LPP influence, along Santa Catarina coast. This regional $\delta^{13}C$ variation pattern could be hypothetically explained by two types of influences superposing that of LPP: the local supply of continental waters through lagoon-estuarine inlets; or the coastal upwelling in the southern limit of the study area. The hypothesis of influence of local freshwater sources on coastal area can be tested by examining previous seawater salinity data. Measurements made by Freitas and Muelbert (2004) in 1995 (spring-summer-fall) in seawater 5 m deep off the inner shelf (up to the 100 m isobath) between Laguna and Cabo Frio indicate lower salinities around the Paranaguá (Paraná State) and Cananeia-Iguape lagoonal-estuarine complexes and the Santos estuary (São Paulo State), with minimum values, recorded near the coast, between 32.5 and 33.0. These values gradually increase up to 35.5 to 36.0 both towards SW (Santa Marta Cape, southern Santa Catarina) and NE (Cabo Frio), as well as to offshore, implying a slight augment of salinity along Santa Catarina coast from north to south. Historical hydrographic data compiled by Piola et al. (2000) to the South America shelf and coastal area between 20° S and 40° S (see also Piola and Romero, 2004) had already demonstrated that salinities lower than 33.0 sometimes registered in this same coastal sector (around latitude 25° S) are more typical of winter, what allowed the authors interpret a northward penetration of low surface temperature waters with substantial contributions of La Plata River. Regardless of the origin of these lower salinity values at latitude 25° S, the fact is that they help to explain the $\delta^{13}C$ results found (Fig. 7), since there is a corresponding $\delta^{13}C$ drop in this sector of the coast (São Paulo and Paraná states). By these reasons, the hypothesis of influence of local freshwater supply on our results (Fig. 7) furnishes a valid explanation for the observed spatial variation pattern of $\delta^{13}C$. The second hypothesis, the influence of coastal upwelling around Santa Marta Cape (Castelão and Barth, 2006), is compatible with the highest vermetids $\delta^{13}C$ values in southern Santa Catarina coast. Higher $\delta^{13}C$ values often found in carbonate shells of upwelling waters can be attributed to two different mechanisms: the first is the enrichment of $\delta^{13}C$ of the inorganic carbon dissolved (DIC) in the water mass and, consequently, of $\delta^{13}C$ of the $CaCO_3$ formed therein, by the increase in primary productivity induced by the upwelling (Ravelo and Hillaire-Marcel, 2007; Sadler et al., 2012; Areias et al., 2020). Regional variations of $\delta^{13}C$ records in vermetids (*Dendropoma petraeum*) detected by Shemesh et al. (2017) between different basins of the Mediterranean Sea were analogously attributed to contrasts of DIC and to the primary productivity of the surface water. The second mechanism is the chemical effect of the lower temperature and/or [$CO_3^{2-}$] of upwelling seawater, which affects the $\delta^{13}C_{shell}$ in an opposite sense and often with a larger magnitude, than the change related to tipically lower $\delta^{13}C_{DIC}$ of this seawater (Peeters et al., 2002; Sadler et al., 2012). In conclusion, the found $\delta^{13}C$ variation pattern (Fig. 7) can be explained not only by the decreasing influence northward of the LPP, but also by the upwelling in southern Santa Catarina and, maybe, by the local continental supply in São Paulo and Paraná lagoon-estuarine systems.

#### 5.2.2. Variation over time

The period of samples absence on Santa Catarina coast between approximately 3.4 and 2.6 cal ka BP and a period of shortage of vermetid samples in the same region after 0.5 cal ka BP (Fig. 2) had already been identified by Baker et al. (2001) as vermetid population decline associated with water cooling in southern Santa Catarina, based on the data of Angulo et al. (1999). Indeed, the grouping of our data with those of Angulo et al. (1999), shown in Fig. 8, evidences that these two periods of vermetid population decline occurred along the entire coast of Santa Catarina. Besides, the first of these two periods, more precisely from 3.3 to 2.7 cal ka BP, can be considered of vermetid decline throughout the São Paulo Embayment (Fig. 8).

The period of vermetid population decline between 3.3 and 2.7 ka BP was preceded by Sr/Ca increasing trend from 5.6 to 3.3 ka BP ($p$ = .20) and followed by Sr/Ca decrease from 2.7 to 0.5 cal ka AP ($p$ = .001; Fig. 2B), which makes possible hypothesizing that there was a Sr/Ca high in coastal waters over this population decline period. Considering that in aragonite mollusks the increase of this elemental ratio may be influenced by decreasing the sea water temperature (Schöne et al., 2011; Roger et al., 2018), a higher Sr/Ca between 3.3 and 2.7 cal ka BP would indicate that coastal water was cooler in this time interval. The period from 5.6 to 3.3 ka BP shows also an increasing trend of $\delta^{18}O$ ($p$ = .006; Fig. 2C). $\delta^{18}O$ in marine mollusk carbonate is of complex interpretation, even more under the influence of freshwater, since it depends as much on the composition of DIC as on the temperature and salinity of the water in which the mollusk have precipitated carbonate (Grossman and Ku, 1986; Ingram et al., 1996; Dettman et al., 1999; Sadler et al., 2012). However, even if a conclusive interpretation cannot be made, the increase of $\delta^{18}O$ found in the vermetids over the period from 5.6 to 3.3 ka BP is compatible with the thermodynamic effect of water decreasing temperature on the biogenic carbonate precipitation and, therefore, coherent with the hypothesis of water cooling, elaborated from the data of Sr/Ca. In the last 0.5 cal ka BP, the Sr/Ca and $\delta^{18}O$ values do not show much significant linear trends (Fig. 2B and C) and more data are required to discuss if this most recent period of vermetid population reduction was accompanied by coastal water cooling.

The most parsimonious explanation for the decrease in water temperature between 3.3 and 2.7 cal ka BP from São Paulo to Santa Catarina coast is the increased influence of cold and fresh water of LPP. The lower temperature and salinity as well as the assumed greater turbidity of LPP can be evoked as possible explanations for the *P. varians* population reduction in the study area. The reason why the periods of vermetid decline were noticed preferentially (from 3.4 to 2.8 ka BP) or only (over the last 0,5 ka BP) in Santa Catarina State may be that the intensity of BCC (and consequently of LPP) decreases northward (Piola et al., 2000, 2005; Sousa & Robinson 2004), being therefore higher in that state than in Paraná and São Paulo. The trend for $\delta^{18}O$ increase during the supposed period of LPP intensification, if related to the thermodynamic effect, indicates that the $\delta^{18}O$ in the studied vermetids carbonate was determined by the water temperature decrease, rather than by water salinity decrease, imposed by LPP. A first reason for this may be that the influence of LPP on coastal water parameters seems to be much stronger in terms of temperature than of salinity. Indeed, nowadays the salinity decrease imposed by LPP's seasonal northward advance, outside the upwelling zone, is around 3.0, while the temperature decrease is about 8 °C (Piola et al., 2000, 2008; Piola and Romero, 2004). Another reason is the great sensitivity of vermetid $\delta^{18}O$ to water temperature variations. According to Antonioli et al. (1999), data obtained from vermetid (*Dendropoma*) specimens collected in Sicily suggest their $\delta^{18}O$ values as a valuable biological indicator of sea surface temperature (SST) trends. For example, in different samples from a same place and of the same species of *Dendropoma* who lived in waters of the same salinity but with a temperature difference of 2 °C, González-Delgado et al. (2005) found a $\delta^{18}O$ average variation of 0.38‰.

Given that the spatial variation of geochemical data (Fig. 7) may be influenced not only by LPP but also by local continental runoff, the possibility of this runoff influence must be also discussed over time. In the study area, continental runoff are directly controlled by SAMS intensity. It influences both the local freshwater and, albeit in a subordinate way, the LPP (Piola et al., 2000; Möller et al., 2008). However, there is a series of reasons to discard the increase of precipitation and continental runoff or SAMS intensification during the periods here interpreted as of greater LPP influence. First, paleoprecipitation high resolution geochemical-isotopic data from Santa Catarina speleothems (Botuverá Cave, 27°S) show relative constancy, at high values, over the last 4 ka (Cruz et al., 2005; Bernal et al., 2016); an intensification of the SAMS, linked to augment of austral summer insolation, and, therefore, an increase of precipitation in great part of southeast South America (Cruz et al., 2005), including the catchment area of the La Plata basin, is better characterized before this, from 7 to 4 ka ago (Bernal et al., 2016; Fig. 9A); second, in another high-resolution reconstruction based on speleothems in southeastern Brazil (Lapa Grande Cave, 14°S), Stríkis et al. (2011) detected low precipitation variations over the same period, except by rapid short-lived increases coincident with Bond events (Fig. 9B), interpreted by the authors as SAMS abrupt intensifications; the period of vermetids decline between 3.3 and 2.7 ka BP occurs between two of these peaks of precipitation and SAMS intensity; third, the period of vermetids population decline from 3.3 to 2.7 ka BP as well as the period of vermetid absence in Santa Catarina State of the last 500 years, both here supposed as increased LPP, can be considered periods of weakening of SAMS, according to data presented by Chiessi et al. (2014) (Fig. 9C and D). These two periods coincide with BC weakening hemicycles identified from the $\delta^{18}O$ of continental-ice-volume-corrected surface seawater ($\delta^{18}O_{ivc\text{-}ssw}$), a proxy for relative sea surface salinity (SSS) derived from *Globigerinoides ruber* geochemical data (Mg/Ca SST and $\delta^{18}O$). According to those authors, periods of weak BC would be, in turn, associated with strengthening of Atlantic Meridional Overturning Circulation (AMOC). Additionally, Chiessi et al. (2014) registered synchrony of periods of strong BC with periods of negative SST anomalies in the high latitudes of the North Atlantic and with positive precipitation anomalies over southeastern South America (Fig. 9B-D).

Thus, precipitation and runoff increases promoted by SAMS strengthening does not seem to be a likely hypothesis for the intensified influence of LPP from 3.3 to 2.7 ka BP and over the last 500 years. The BCC strengthening during the moments of weakened BC, and therefore weakened NNE winds and strengthened AMOC (Chiessi et al., 2014), is a more suitable interpretation.

Nagai et al. (2020) inferred the latitudinal SST gradient (BC strength) in two piston-cores in Paraná State offshore (25.5°S, 46.6°W, 89 m water depth, and 25.0°S, 45.6°W, 100 m water depth) based on Mg/Ca data of *G. ruber* (pink) from 6 ka to 1 ka BP. The authors compared the intensity of BC (Fig. 9E) with the intensity of BCC indicated by Ti/Ca ratios obtained by Mahiques et al. (2009) from core sediments of the Santa Catarina shelf (27°S, 60 m water depth; Fig. 9F). This comparison shows that fluctuations of BCC and BC are inversely related, mainly after circa 2.8 ka BP, when modern climatic conditions regarding wind regime and precipitation would have been established over southeast South America, favoring the LPP action over this portion of São Paulo Embayment (Mahiques et al., 2009; Nagai et al., 2020).

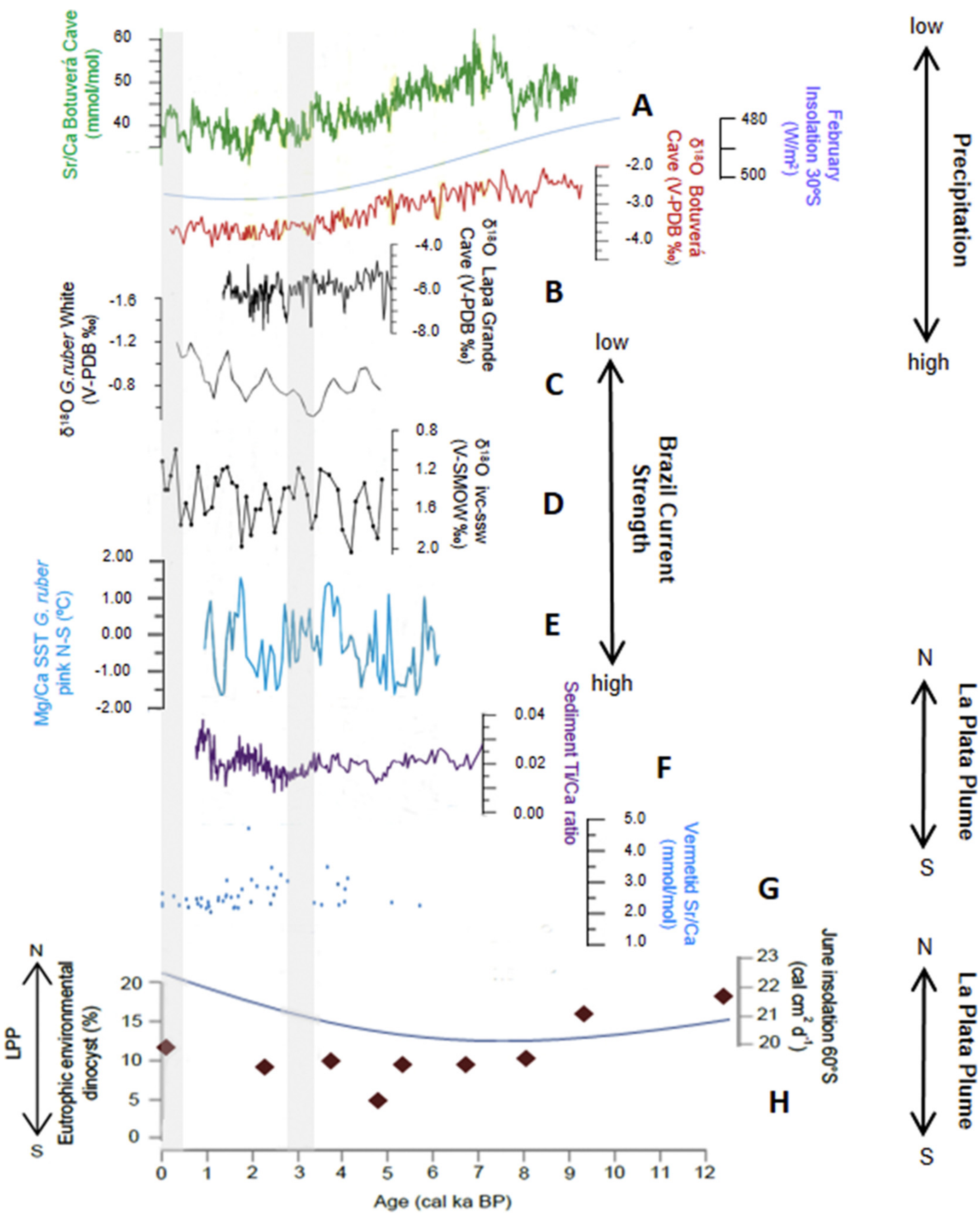


**Fig. 9.** Comparison between different proxies for paleoclimate in the continental and marine south/southeastern Brazil. A: Sr/Ca ratio and δ$^{18}$O from stalagmite BT2 (Botuverá, Santa Catarina State), compared with austral summer (February) insolation at 30°S (Bernal et al., 2016); B: δ$^{18}$O from composite stalagmite LG3/LG11 collected in central-eastern Brazil at 14.42°S/44.37°W (Stríkis et al., 2011); C: three-point running average of *Globigerinoides ruber* white δ$^{18}$O from marine sediment core GeoB2107–5 collected in the western South Atlantic at 27.18°S/46.46°W (Chiessi et al., 2014); D: ice volume corrected (ivc) surface seawater (ssw) δ$^{18}$O from composite marine sediment core GeoB6211–1/2 collected in the western South Atlantic at 32.51°S/50.24°W (Chiessi et al., 2014); E: latitudinal SST gradient, north less south (N-S), based on the Mg/Ca ratio of *G. ruber* (pink) from cores 7616, collected at 25.0°S, 45.6°W, and 7610, at 25.5°S, 46.6°W (Nagai et al., 2020); F. Ti/Ca ratios, core 7606, 27°S (Nagai et al., 2020 with data from Mahiques et al., 2009). G: Sr/Ca values of 50 vermetid samples from São Paulo (SP), Paraná (PR) and Santa Catarina (SC) states (this work); H: abundance of dinoflagellate cysts from core GeoB2107–3 (27°S) (Portilho-Ramos et al., 2019 with data from Gu et al., 2017) and austral winter (June) insolation at 60°S (Berger and Loutre, 1991). Gray bars represent the periods of vermetid scarcity between 3.3 and 2.7 cal ka BP (São Paulo Embayment) and 0.5–0 cal ka BP (SC). (For interpretation of the references to colour in this figure legend, the reader is referred to the web version of this article.)

The first period of scarce vermetids, which occurred immediately before this supposed transition to modern conditions, is marked by three successive peaks of BC weakening (in theory, strengthening of the BCC, coherently with our interpretation to vermetids data; Fig. 9E and G), but with low Ti/Ca (interpreted in Fig. 9F as weakening of LPP, differently of our interpretation). The low Ti/Ca values in this period, on the other hand, are consistent with the idea of BC weakening (Figs. 9C-E), assuming the direct relationship of BC with intensification of SAMS, precipitation and terrigenous supply. In addition, they can be better understood if other climatic-oceanographic mechanisms potentially controlling BCC are considered.

Among these other mechanisms, one of the most explicitly evoked in the scarce previous studies about BCC (Campos et al., 1999, 2008; Gyllencreutz et al., 2010) is the variability of El Niño Southern Oscillation (ENSO) at millennial timescales (Moy et al., 2002; Rein et al., 2005; Jara et al., 2015, 2019; Mariani et al., 2017), including the onset of the modern ENSO in the beginning of Late Holocene. The coincidence between high discharge events of the Paraná River, the main affluent of La Plata River, and equatorial Pacific SST anomalies typical of ENSO events (Depetris et al., 1996) led Campos et al. (1999) to interpret a relation between El Niño events, precipitation over South America and anomalies in the BCC. However, as El Niño events are accompanied by winds from NNE, the maximum northward advances of BCC, carrying the LPP, do not coincide with them but with the low discharge regime typical of La Niña events (Piola et al., 2005; Möller et al., 2008). As effect, El Niño high discharge years are characterized by offshore displacement and southwestward retreat of LPP, while La Niña lower discharge years favor SSE winds and northward advance of LPP (Campos et al., 2008). Thus, intensification moments of the BCC, with expansion of the LPP reach to the north, could be associated with strengthening of the ENSO amplitude under a La Niña dominant condition. Gyllencreutz et al. (2010), with base on sedimentary record of three cores along south-southeast Brazilian margin proposed an event of these, resulting in a net increase in northward transport up to at least 25°S, around 3–2 cal ka BP. Meanwhile, Barr et al. (2019) found simultaneous evidences in Galápagos and eastern Australia sedimentary records of a centennial-scale period of enhanced zonal SST gradient, with a more La Niña-like mean state around 3.5–3.0 cal ka BP. This period is nearly coincident with the time interval of decline of vermetids in south-southeast Brazilian coast here attributed to an intensified BCC. Jara et al. (2015), based on paleofloristic records over New Zealand, interpret more frequent El Niño states from 2.7 ka BP, coinciding with the resumption of the vermetids on the São Paulo Embayment coast.

Zular et al. (2013) proposed the intensification of the southerly winds (responsible for transporting BCC) after 2 ka BP, based on changes in the coastal morphodynamics and sedimentological provenance at São Francisco do Sul (Santa Catarina State). This intensification, according to them could result from a northbound shift of the westerlies wind belt coupled with the intensification of ENSO events.

Another hypothesis to LPP variability is presented by Portilho-Ramos et al. (2019), who recognized a close connection between dinocyst abundance and austral winter insolation (at 60°S) in a marine core located at 27°S over the last 70 ka and interpreted that the periods of increased insolation led to increase of the thermal gradient between the high- and mid-latitudes in the Atlantic sector of the Southern Ocean, and, consequently, to intensification of alongshore southwesterly wind system and the northward incursion of LPP (Fig. 9H). Data obtained by these authors are suggestive of an inhibiting of the northward intrusions of the LPP in the post-glacial. Despite this, and admitting the relation proposed by them, it is possible to hypothesize that the end of the decreasing trend of 60°S June insolation in the Early to Middle Holocene (Fig. 9H) has promoted a climatic-oceanographic setting more favorable to the BCC intensification. The scarcity of Holocene data from Portilho-Ramos et al. (2019), however, does not allow verifying this hypothesis nor properly compare their results with the ones presented in this work.

The inverse correlation of BCC with BC, the influence on BCC of the millenary variability of ENSO and the intensification of BCC over the last few millennia due to increasing trend of 60° S June insolation are three hypotheses, not mutually exclusive, that can help to explain the vermetids decline in Sao Paulo Embayment at some stages of Late Holocene. The assessment of the feasibility of each of these hypotheses, however, depends on further specific studies on BCC being carried out in the future.

## 6. Conclusions

The RSL variation curve obtained for the northern coast of Santa Catarina State reveals similar behavior with the curve presented by previous works for the southern coast of the same state, that is smooth trend of sea level fall along all the Late Holocene. The data present here also point to slight differences in the behavior of RSL variation curve from Santa Catarina state to the further northern locations, although more paleo-sea level measurements are required to understand the real extension of latitudinal differences between sea level variation curves along Brazilian coast and therefore allow the construction of more accurate models of regional hydro-isostatic adjustments for the Late Holocene.

The vermetid colony collected in the top of a vertical narrow cavity presents higher altitude than the samples of similar age, meaning that better descriptions of the bedrock morphology, wave exposure and oceanographic conditions, as tidal and wave regime can improve the precision of paleo-sea level reconstructions. It would be also necessary to quantify the living vertical vermetid distribution under these different conditions and this approach may also be applied for other species used as paleo-sea level indicators.

LPP alone is not sufficient to explain the spatial variation pattern of average values of $\delta^{13}C$. The larger supply of fresh water by estuarine-lagoon systems (Santos, Iguape-Cananeia and Paranaguá) is a possible explanation to the lower average $\delta^{13}C$ values in São Paulo and Paraná states, whereas more enriched average values of $\delta^{13}C$ found in southern Santa Catarina State may be related to the phenomenon of coastal upwelling that occurs around Santa Marta Cape.

Sr/Ca and $\delta^{18}O$ data suggest variations in the physicochemical parameters of coastal water, at regional scale, which can be generated by variation in the intensity of the BCC in the upper Holocene, whose strengthening may have been responsible for the population decline of *P. varians* in São Paulo Embayment at 3.3–2.7 cal ka BP and in Santa Catarina over the last 0.5 cal ka BP.

## Declaration of Competing Interest

The authors declare that they have no known competing financial interests or personal relationships that could have appeared to influence the work reported in this paper.

## Acknowledgements

The authors are grateful to Dr. Francisco W. da Cruz Junior and Alyne Barros, for the analyses in the Laboratório de Isótopos Estáveis of the Universidade de São Paulo, Brazil; to Isaac J. Sayeg, Jordana A. Zampelli and Luciana Nogueira, for the technical support in laboratory work; to Thaís A. da Silva, for the help with the drawings; to Hílton G. Fernandes, for the statistical consultancy; and to Dr. Gert De Lange and two anonymous reviewers for their suggestions and comments that contribute to improve this manuscript. This research was supported by: the São Paulo Research Foundation (FAPESP) (PCFG, Process Number: 09/54232-4 and TFT scholarship, Process Number: 13/21941-8); the National Council for Scientific and Technological Development (CNPq) (PCFG, Process Numbers: 308772/2018-0 and 428341/2018-7; RJA, Process Number: 477945/2012-0; LCRP Process Number: 2017/03304-1); the Fundação Araucária (RJA, senior grant 45725); and the Programa Nacional de Pós-Doutorado / Coordenação de Aperfeiçoamento de Pessoal de Nível Superior - PNPD/CAPES (PSO, Process Number: 88887.320380/2019-00).

## References

Almeida, F.F.M., 1964. Os fundamentos geológicos do relevo paulista. In: Boletim do Instituto Geográfico e Geológico. 41. pp. 169–263.
Almeida, F.F.M., Carneiro, C.D.R., 1998. Origem e evolução da Serra do Mar. Revista Brasileira de Geociências 28 (2), 135–150.
Angulo J., Rodolfo, Lessa C., Guilherme, Souza C., Maria, 2009. The Holocene barrier systems of Paranaguá and northern Santa Catarina coasts, Southern Brazil. In: Dillenburg R.Sérgio, Hesp A.Patrick (Eds.), Geology and Geomorphology of Holocene Coastal Barriers of Brazil. Springer-Verlag, Berlin, pp. 135–176.
Angulo, R.J., Souza, M.C., 2014. Revisão conceitual de indicadores costeiros de paleoníveis marinhos quaternários no Brasil. Quat. Environ. Geosci. 5 (2), 01–32.
Angulo, R.J., Giannini, P.C.F., Suguio, K., Pessenda, L.C.R., 1999. Relative Sea-level

changes in the last 5500 years in southern Brazil (Laguna-Imbituba region, Santa Catarina State) based on vermetid 14C ages. Mar. Geol. 159, 323–339.
Angulo, R.J., Lessa, G.C., Souza, M.C., 2006. A critical review of mid- to late-Holocene Sea-level fluctuations on the eastern Brazilian coastline. Quate. Sci. Rev. 25, 486–506.
Angulo, R.J., Souza, M.C., Fernandes, L.A., Disaró, S.T., 2015. Quaternary Sea-level changes and aeolianites in the Fernando de Noronha archipelago, northeastern Brazil. Quat. Int. 305, 15–30.
Angulo, R.J., Souza, M.C., Dillenburg, S.R., Barboza, E.G., Rosa, M.L.C.C., 2020. Late-Holocene sea-level fall after eustatic sea-level maximum at 28°S latitude, southern Brazil.
Antonioli, F., Chemello, R., Improta, S., Riggio, S., 1999. Dendropoma lower intertidal reef formations and their palaeoclimatological significance, NW Sicily. Mar. Geol. 161, 155–170.
Areias, C., Spotorno-Oliveira, P., Bassic, D., Iryu, Y., Nashe, M., Castro, J.W.A., Tâmega, F.T.S., 2020. Holocene Sea-surface temperatures and related coastal upwelling regime recorded by vermetid assemblages, southeastern Brazil (Arraial do Cabo, RJ). Mar. Geol. 425.
Baker, R.G.V., Haworth, R.J., Flood, P.G., 2001. Warmer or cooler late Holocene marine palaeoenvironments?: interpreting southeast Australian and Brazilian sea-level changes using fixed biological indicators and their $^{18}$O composition. Palaeogeogr. Palaeoclimatol. Palaeoecol. 168, 249–272.
Barr, C., Tibby, J., Leng, M.J., Tyler, J.J., Henderson, A.C.G., Overpeck, J.T., Simpson, G.L., Cole, J.E., Phipps, S.J., Marshall, J.C., Mcgregor, G.B., Hua, Q., Mcrobie, F.H., 2019. Holocene El Niño–Southern Oscillation variability reflected in subtropical Australian precipitation. Sci. Rep. 9, 1627.
Benetti, M., Reverdin, G., Aloisi, G., Sveinb, A., 2017. Stable isotopes in surface waters of the Atlantic Ocean: Indicators of ocean-atmosphere water fluxes and oceanic mixing processes. J. Geophys. Res. Oceans 122, 4723–4742.
Berger, A., Loutre, M.F., 1991. Insolation values for the climate of the last 10 million years. Quat. Sci. Rev. 10 (4), 297–317.
Bernal, J.P., Cruz, F.W., Stríkis, N.M., Wang, X., Deininger, M., Catunda, M.C.A., Ortega-Obregón, C., Cheng, H., Edwards, R.L., Auler, A.S., 2016. High-resolution Holocene South American Monsoon history recorded by a speleothem from Botuverá cave, Brazil. Earth Planet. Sci. Lett. 450, 186–196.
Breves, A., Széchy, M.T.M., Lavrado, H.P., Junqueira, A.O., 2017. Abundance of the reef-building Petaloconchus varians (Gastropoda: Vermetidae) on intertidal rocky shores at Ilha Grande Bay, southeastern Brazil. An. Acad. Bras. Cienc. 89 (2), 907–918.
Butler, L.W., 1970. Shallow structure of the continental margin, southern Brazil and Uruguay. Geol. Soc. Am. Bull. 81 (4), 1079–1096.
Campos, E.J.D., Lentini, C.D., Miller, J.L., Piola, A.R., 1999. Interannual variability of the sea surface temperature in the South Brazil Bight. Geophys. Res. Lett. 26, 2061–2064.
Campos, E.J.D., Piola, A.R., Matano, R.P., Miller, J.L., 2008. Editorial: PLATA: A synoptic characterization of the Southwest Atlantic shelf under influence of the Plata River and Patos Lagoon outflows. Cont. Shelf Res. 28 (13), 1551–1555.
Campos, P.C., Moller, O., Piola, A.R., Palma, E.D., 2013. Seasonal variability and coastal upwelling near Cape Santa Marta (Brazil). J. Geophys. Res. 118 (3), 1420–1433. https://doi.org/10.1002/jgrc.20131.
Castelão, R.M., Barth, J.A.C., 2006. Upwelling conditions around Cabo Frio, Brazil: the importance of wind stress curl. Geophys. Res. Lett. 33 (L03062). https://doi.org/10.1029/2005GL025182.
Chanton, J.P., Lewis, F.G., 1999. Plankton and Dissolved Inorganic Carbon Isotopic Composition in a River-Dominated Estuary: Apalachicola Bay, Florida. Estuaries 22, 575–583.
Chemello, R., Silenzi, S., 2011. Vermetid reefs in the Mediterranean Sea as archives of sea-level and surface temperature changes. Chem. Ecol. 27, 121–127.
Chiessi, C.M., Mulitza, S., Groeneveld, J., Silva, J.B., Campos, M.C., Gurgel, M.H., 2014. Variability of the Brazil current during the late Holocene. Palaeogeogr. Palaeoclimatol. Palaeoecol. 415, 28–36.
Colonese, A.C., Netto, S.A., Francisco, A.S., Deblasis, P., Villagran, X.S., De Ponzoni, R.A.R., Hancock, Y., Hausmann, N., Eloy De Farias, D.S., Prendergast, A., Schöne, B.R., Cruz, F.W., Giannini, P.C.F., 2017. Shell sclerochronology and stable isotopes of the bivalve Anomalocardia flexuosa (Linnaeus, 1767) from southern Brazil: Implications for environmental and archaeological studies. Palaeogeogr. Palaeoclimatol. Palaeoecol. 484, 7–21.
Cruz, F.W., Burns, S.J., Karmann, I., Sharp, W.D., Vuille, M., Cardoso, A.O., Ferrari, J.A., Dias, P.L.S., Viana, O., 2005. Insolation-driven changes in atmospheric circulation over the past 116,000 years in subtropical Brazil. Nature 434, 63–65.
Dahiru, T., 2008. P – value, a true test of statistical significance? A cautionary note. Ann. Ib. Postgrad. Med. 6 (1), 21–26.
Delibrias, C., Laborel, J., 1969. Recent variations of the sea level along the Brazilian coast. Quaternaria 14, 45–49.
Depetris, P.J., Kempes, S., Latif, M., Mook, W.G.., 1996. ENSO-controlled flooding in the Paraná River (1904-1991). Naturwissenschaften 83, 127–129.
Dettman, D.L., Reische, A.K., Lohmann, K.C., 1999. Controls on the stable isotope compositionof seasonal growth bands in aragonitic fresh-water bivalves (Unionidae). Geochim. Cosmochim. Acta 63, 1049–1057.
Dominguez, J.M.L., 2009. The coastal zone of Brazil. In: Dillenburg, S.R., Hesp, P.A. (Eds.), Geology and Geomorphology of Holocene Coastal Barriers of Brazil. Springer, Berlin – Heidelberg, pp. 17–51.
Donnarumma, L., Sandulli, R., Appolloni, L., Di Stefano, F., Russo, G.F., 2018. Morpho-structural and ecological features of a shallow vermetid bioconstruction in the Tyrrhenian Sea (Mediterranean Sea, Italy). J. Sea Res. 131, 61–68.
Emílsson, I., 1956. Relatório e resultados físico-químicos de três cruzeiros oceanográficos em 1956. Contr. Avul. Inst. Ocean., Oceanografia Física 1, 1–70.
Emílsson, I., 1961. The shelf and coastal waters off southern Brazil. Publ. do Inst. Ocean. da USP, n. 144, 101–112.
Franchito, S.H., Oda, T.O., Brahmananda Rao, V., Kayan, M.T., 2008. Interaction between coastal upwelling and local winds at Cabo Frio, Brazil: an observational study. J. Appl. Meteorol. Climatol. 47, 1590–1598.
Freitas, D.M., Muelbert, J.H., 2004. Ichthyoplankton distribution and abundance off southeastern and southern Brazil. Braz. Arch. Biol. Technol. 47 (4), 601–612. https://doi.org/10.1590/S1516-89132004000400014.
Fukumoto, M.M., Mahiques, M.M., Tessler, M.G., 2004. Bottom faciology and sediment transport in Santos Bay, Southeastern Brazil. J. Coast. Res. SI39, 1737–1740.
Garreaud, R.D., Vuille, M., Compagnucci, R., Marengo, J., 2009. Present-day south American climate. Palaeogeogr. Palaeoclimatol. Palaeoecol. 281, 180–195.
Giannini, P.C.F., Guedes, C.C.F., Nascimento, D.R., Tanaka, A.P.B., Angulo, R.J., Assine, M.L., Souza, M.C., 2009. Morphology and sedimentology of Ilha Comprida, southern São Paulo coast. In: Dillenburg, S.R., Hesp, P.A. (Eds.), Geology and Geomorphology of Holocene Coastal Barriers of Brazil. Springer, Berlin – Heidelberg, pp. 177–224.
González-Delgado, J.A., Zazo, C., Goy, J.L., Civis, J., Templado, J., M, C.A.L.V.O., Dabrio, C.J., 2005. Paleoenvironmental significance of C and O isotopic signal in Last Interglacial gastropod Dendropoma shell concentrations from Canary (Spain) and Sal (Cape Verde) islands. Rev. Soc. Geol. Esp. 18 (3–4), 207–211.
Grossman, E.L., Ku, T.-L., 1986. Oxygen and carbon isotope fractionation in biogenic aragonite: temperature effects. Chem. *Geol. Isot. Geosci.* 59, 59–74.
Gu, F., Zonneveld, K.A., Chiessi, C.M., Arz, H.W., Pätzold, J., Behling, H., 2017. Long-term vegetation, climate and ocean dynamics inferred from a 73,500 years old marine sediment core (GeoB2107-3) off southern Brazil. Quat. Sci. Rev. 172, 55–71.
Gyllencreutz, R., Mahiques, M.M., Alves, D.V.P., Wainer, I.K.C., 2010. Mid- to late-Holocene paleoceanographic changes on the southeastern Brazilian shelf based on grain size records. The Holocene 20, 863–875.
Hesp, P.A., Giannini, P.C.F., Martinho, C.T., Miot Da Silva, G., Asp Neto, N.E., 2009. The Holocene barrier system of the Santa Catarina coast, Southern Brazil. In: Dillenburg, S.R., Hesp, P.A. (Eds.), Geology and Geomorphology of Holocene Coastal Barriers of Brazil. Springer, Berlin – Heidelberg, pp. 93–134.
Ingram, B.L., Conrad, M.E., Ingle, J.C., 1996. Stable isotope and salinity systematics in estuarine waters and carbonates: San Francisco Bay. Geochim. Cosmochim. Acta 60 (3), 455–467.
Jacobson, Y., Yam, R., Montagna, P., López Correa, M., Devoti, S., Shemesh, A., 2017. Trace elements of Mediterranean vermetid reefs as proxies for natural and anthropogenic processes. Goldschmidt2017 Abstract. pp. 35.
Jara, I.A., Newnham, R.M., Vandergoes, M.J., Foster, C.R., Lowe, D.J., Wilmshurst, J.M., Moreno, P.I., Renwick, J.A., Homes, A.M., 2015. Pollen–climate reconstruction from northern South Island, New Zealand (41°S), reveals varying high- and low-latitude teleconnections over the last 16 000 years. J. Quat. Sci. 30 (8), 817–829.
Jara, I.A., Maldonado, A., González, L., Hernández, A., Sáez, A., Giralt, S., Bao, R., Valero-Garcés, B., 2019. Centennial-scale precipitation anomalies in the southern Altiplano (18°S) suggest an extratropical driver for the South American summer monsoon during the late Holocene. Climate Past 15, 1845–1859.
Keen, A.M., 1961. A proposed reclassification of the gastropod family Vermetidae. Bull. Br. Museum (Natural History) Zool. 7, 183–213.
Laborel, J., 1977. Are reef building vermetid disappearing in the South Atlantic? Proc. Int. Coral Reef Symposium 3, 233–237.
Laborel, J., 1979. Fixed marine organisms as biological indicator for the study of recent sea level and climatic variations along the Brazilian tropical coast. In: Proc. Int. Symp. On: Coastal Evolution in the Quaternary, São Paulo, 1978. Proceedings, São Paulo, IGCP/Project 61, Instituto de Geociências. Universidade de São Paulo, pp. 193–211.
Laborel, J., 1986. Vermetid gastropods as sea-level indicators. In: Van de Plaasche, O. (Ed.), Sea Level Research, a Manual for the Collection and Evaluation of Data. 12. Geo Books, Norwich, pp. 281–310.
Laborel, J., Laborel-Deguen, F., 1996. Biological indicators of Holocene Sea level and climatic variations on rocky coasts of tropical and subtropical regions. Quat. Int. 31, 53–60.
Mahiques, M.M., Wainer, I.K.C., Burone, L., Nagai, R., Sousa, S.H.D.M., Figueira, R.C.L., Hammer, Ø., 2009. A high resolution Holocene record on the southern Brazilian shelf: paleoenvironmental implications. Quat. Int. 206, 52–61.
Mariani, M., Fletcher, M., Dysdale, R.N., Saunders, K.M., Heijnis, H., Jacobsen, G., Zawadzki, A., 2017. Coupling of the intertropical convergence zone and southern hemisphere mid-latitude climate during the early to mid-Holocene. Geology 45 (12), 1083–1086.
Mazzini, P.L.F., Barth, J.A., 2013. A comparison of mechanisms generating vertical transport in the Brazilian coastal upwelling regions. J. Geophys. Res. 118, 5977–5993.
Möller, O.O., Piola, A.R., Freitas, A.C., Campos, E.J.D., 2008. The effects of river discharge and seasonal winds on the shelf off southeastern South America. Cont. Shelf Res. 28, 1607–1624.
Mook, W.G., Tan, F.C., 1991. Stable carbon isotopes in rivers and estuaries. In: Degens, E.T., Kempe, S., Richey, J.E. (Eds.), Biogeochemistry of Major World Rivers. John Wiley and Sons, Chichester, UK, pp. 245–264.
Moy, C.M., Seltzer, G.O., Rodbell, D.T., Anderson, D.M., 2002. Variability of El Niño/Southern Oscillation activity at millennial timescales during the Holocene epoch. Nature 420, 162–164.
Nagai, R.H., Chiessi, C.M., Kuhnert, H., Sousa, S.H., Wainer, I.E., Figueira, R.C., Mahiques, M.M., 2020. South Brazilian Bight mid-to late Holocene hydrographic fluctuations. Geo-Mar. Lett. 1–11.
Newton, R., Bottrell, S., 2007. Stable isotopes of carbon and Sulphur as indicators of environmental change: past and present. J. Geol. Soc. 164 (4), 691–708.
Palma, E.D., Matano, R.P., 2009. Disentangling the upwelling mechanisms of the South Brazil Bight. Cont. Shelf Res. 29, 1525–1534.

Peeters, F.J.C., Brummer, G.J.A., Ganssen, G., 2002. The effect of upwelling on the distribution and stable isotope composition of Globigerina bulloides and Globigerinoides ruber (planktic foraminifera) in modern surface waters of the NW Arabian Sea. Glob. Planet. Chang. 34 (3–4), 269–291.

Pianca, C., Mazzini, P.L.F., Siegle, E., 2010. Brazilian offshore wave climate based on NWW3 reanalysis. Braz. J. Oceanogr. 58 (1), 53–70.

Pierre, C., Vergnaud-Grazzini, C., Faugeres, J.C., 1991. Oxygen and carbon stable isotope tracers of the water masses in the Central Brazil Basin. Deep-Sea Res. 38 (5), 597–606.

Piola, A.R., Romero, S.I., 2004. Analysis of space-time variability of the Plata River plume. Gayana (Concepc.) online 68 (2), 482–486.

Piola, A.R., Campos, E.J.D., Möller, O.O., Charo, M., Martinez, C., 2000. Subtropical shelf front off eastern South America. J. Geophys. Res. 105, 6565–6578.

Piola, A.R., Matano, R.P., Palma, E.D., Moller, J.R., Campos, E.J., 2005. The influence of the Plata River discharge on the western South Atlantic shelf. Geophys. Res. Lett. 32 (1), 1–4.

Piola, A.R., Romero, S.I., Zajaczkovski, U., 2008. Space-time variability of the Plata plume inferred from ocean color. Cont. Shelf Res. 28 (13), 1556–1567.

Portilho-Ramos, R.D.C., Pinho, T.M.L., Chiessi, C.M., Barbosa, C.F., 2019. Understanding the mechanisms behind high glacial productivity in the southern Brazilian margin. Clim. Past 15 (3), 943–955.

Ravelo, A.C., Hillaire-Marcel, C., 2007. Chapter eighteen: the use of oxygen and carbon isotopes of foraminifera in Paleoceanography. Dev. Marine Geol. 1, 735–764.

Razik, S., Chiessi, C.M., Romero, O.E., Von Dobeneck, T., 2013. Interaction of the South American Monsoon System and the Southern Westerly Wind Belt during the last 14 kyr. Palaeogeogr. Palaeoclimatol. Palaeoecol. 374, 28–40.

Rein, B., Lückge, A., Reinhardt, L., Sirocko, F., Wolf, A., Dullo, W.-C., 2005. El Niño variability off Peru during the last 20,000 years. Paleoceanography 20, PA4003.

Roger, L.M., George, A.D., Shaw, J., Hart, R.D., Roberts, M.P., Becker, T., Evans, N.J., Mcdonald, B.J., 2018. Geochemical and crystallographic study of Turbo torquatus (Mollusca: Gastropoda) from southwestern Australia. Geochem. Geophys. Geosyst. 19, 214–231. https://doi.org/10.1002/2017GC007287.

Sadler, J., Carré, M., Azzoug, M., Schauer, A.J., Ledesma, J., Cardenas, F., Chase, B.M., Bentaleb, I., Muller, S.D., Mandeng, M., Rohling, E.J., Sachs, J.P., 2012. Reconstructing past upwelling intensity and the seasonal dynamics of primary productivity along the Peruvian coastline from mollusk shell stable isotopes. Geochem. Geophys. Geosyst. 13, 1): 1–17. Q01015. https://doi.org/10.1029/2011GC003595.

Safriel, U., 1966. Recent vermetid formation on the Mediterranean shore of Israel. Proc. Malac. Soc. Lond. 37 (1966), 27–34.

Schettini, C.A.F., 2002. Caracterização física do estuário do rio Itajaí-Açu, SC. *RBRH – Revista Brasileira de*. Recursos Hídricos 7 (1), 123–142.

Schöne, B.R., Zhan, Z., Radermacher, P., Thébault, J., Jacob, D.E., Nunn, E.V., Murer, A.-F., 2011. Sr/Ca and Mg/Ca ratios of ontogenetically old, long-lived bivalve shells (*Artica islandica*) and their function as paleotemperature proxies. Palaeogeogr. Palaeoclimatol. Palaeoecol. 302, 52–64.

Shemesh, A., Yam, R., Jacobson, Y., López Correa, M., Devoti, S., Montagna, P., 2017. The stable isotope record of vermetids from the Eastern, Central and Western Mediterranean basins during the past two millennia. Goldschmidt2017 Abstract. pp. 23.

Silenzi, S., Antonioli, F., Chemello, R., 2004. A new marker for sea surface temperature trend during the last centuries in temperate areas: vermetid reef. Glob. Planet. Chang. 40, 105–114.

Silveira, I.C.A., Schmidt, A.C.K., Campos, E.J.D., Godoi, S.S., Ikeda, Y., 2000. A Corrente do Brasil ao largo da costa leste brasileira. Rev. Bras. Oceanogr. 48, 171–183.

Souza, R.B., Robinson, I.S., 2004. Lagrangian and satellite observations of the Brazilian Coastal Current. Cont. Shelf Res. 24, 241–262.

Spotorno-Oliveira, P., Tâmega, F.T.S., Bemvenuti, C.E., 2012. An overview of the recent vermetids (Gastropoda: Vermetidae) from Brazil. Strombus 19, 1–8.

Spotorno-Oliveira, P., Tâmega, F.T.S., Oliveira, C.A., Castro, J.W.A., Coutinho, R., Iryu, Y., Bassi, D., 2016. Effects of Holocene Sea level changes on subtidal palaeoecosystems, southeastern Brazil. Mar. Geol. 381, 17–28.

Stríkis, N.M., Cruz, F.W., Cheng, H., Karmann, I., Edwards, R.L., Vuille, M., Wang, X., Paula, M.S., Novello, V.F., Auler, A.S., 2011. Abrupt variations in South American monsoon rainfall during the Holocene based on a speleothem record from Central-Eastern Brazil. Geology 39, 1075–1078.

Venancio, I.M., Belem, A.L., Santos, T.H.R., Zucchi, M.R., Azevedo, A.E.G., Capilla, R., Albuquerque, A.L.S., 2014. Influence of continental shelf processes in the water mass balance and productivity from stable isotope data on the Southeastern Brazilian coast. J. Mar. Syst. 139, 241–247.

Vera, C., Higgins, W., Amador, J., Ambrizzi, T., Garreaud, R., Gochis, D., Gutzler, D., Lettenmaier, D., Marengo, J., Mechoso, C.R., Nogues-Paegle, J., Silva-Dias, P.L., Zhang, C., 2006. Towards a unified view of the American Monsoon System. J. Clim. 19, 4977–5000.

Villwock, J.A., Lessa, G.C., Suguio, K., Angulo, R.J., Dillenburg, S.R., 2005. Geologia e Geomorfologia de Regiões Costeiras. In: Souza, C.R.G. (Ed.), Quaternário do Brasil. Ribeirão Preto, Holos Editora, pp. 94–113.

Zular, A., Sawakuchi, A.O., Guedes, C.C.F., Mendes, V.R., Nascimento, D.R., Giannini, P.C.F., Aguiar, V.A.P., Dewitt, R., 2013. Late Holocene intensification of colds fronts in southern Brazil as indicated by dune development and provenance changes in the São Francisco do Sul coastal barrier. Mar. Geol. 335, 64–77.